Temporally precise labeling and control of neuromodulatory circuits in the mammalian brain

Dongmin Lee[1,2,7], Meaghan Creed[3,6,7], Kanghoon Jung[1,7], Thomas Stefanelli[3], Daniel J Wendler[1], Won Chan Oh[1], Neymi Layne Mignocchi[1], Christian Lüscher[3,4] & Hyung-Bae Kwon[1,5]

Few tools exist to visualize and manipulate neurons that are targets of neuromodulators. We present *i*Tango, a light- and ligand-gated gene expression system based on a light-inducible split tobacco etch virus protease. Cells expressing the *i*Tango system exhibit increased expression of a marker gene in the presence of dopamine and blue-light exposure, both *in vitro* and *in vivo*. We demonstrated the *i*Tango system in a behaviorally relevant context, by inducing expression of optogenetic tools in neurons under dopaminergic control during a behavior of interest. We thereby gained optogenetic control of these behaviorally relevant neurons. We applied the *i*Tango system to decipher the roles of two classes of dopaminergic neurons in the mouse nucleus accumbens in a sensitized locomotor response to cocaine. Thus, the *i*Tango platform allows for control of neuromodulatory circuits in a genetically and functionally defined manner with spatial and temporal precision.

A long-standing question in modern neuroscience is how neural-circuit function mediates complex behaviors. Understanding of the neuronal circuitry underlying specific behaviors or brain diseases has expanded tremendously in recent years. In particular, monitoring neuronal activity *in vivo* with genetically encoded calcium indicators and genetic labeling of an active population of neurons (for example by using the immediate early genes Arc (also known as Arg3.1) and c-fos) have enabled the first exploration of real-time activity changes and the circuit basis of behaviors[1–4]. However, there is a lack of effective techniques to convert neuromodulatory actions into gene expression, although visualization of behaviorally relevant neuromodulation-sensitive neurons in a temporally and spatially precise manner is critical to understanding the diversity of animal behavior, sensation, and cognitive functions[5–7].

Tango is a genetic method of labeling cells that have been exposed to a ligand. The system couples a bacterial transcription factor (e.g., lexA) to the exogenous domain of a receptor via a specific tobacco etch virus (TEV) protease–sensitive cleavage site. A Tango mapping system that detects the presence of specific neuromodulators (notably dopamine) has been developed over the past several years[8–10]. The system was originally designed to monitor metabotropic G-protein-coupled-receptor activation[8], but it has also been used to map neuromodulation in *Drosophila*[9,10], examine lipid metabolism[11], and perform drug screens of human G-protein-coupled receptors[12]. However, technical limitations of this system, including high background signal, poor signal-to-noise ratio (SNR), and the inability of specific antagonists to block ligand-induced gene expression[9], have limited the use of this technique for studying neuromodulatory states in mammals *in vivo*. Methods of studying neuromodulation with high temporal and spatial resolution, and techniques that allow for inducible and reversible control of gene expression in animals, are critical for studying neuronal plasticity or neural circuits underlying animal behavior[13–19]. Here, we report the development of a technique for converting neuromodulatory-ligand binding events into gene expression with high temporal fidelity and SNR. To do so, we designed an inducible Tango (*i*Tango)-based system that is switched on by light, such that gene expression is induced only in cells receiving coincident stimulation with ligand and light.

RESULTS

Development of a blue-light-inducible TEV protease system

We created a two-component light-switch control system, named blue-light-inducible TEV protease (BLITz; **Fig. 1a**), consisting of two synthetic proteins and a single reporter vector with a tetracycline response element (TRE). The first component is a membrane-tethered synthetic protein consisting of multiple light-sensitive modules: CIBN (a truncated form of cryptochrome-interacting basic-helix-loop-helix 1)[20]; TEV-N (the N-terminal region of TEV)[21]; TEV protease–cleavage sequence (TEVseq) inserted in a truncated form of *Avena sativa* phototropin1 light-oxygen-voltage 2 domains (AsLOV2)[22]; and TetR-VP16 (a tetracycline-controlled transcriptional activator (tTA)) (**Fig. 1a**). The second component is a fusion protein of TEV-C (C-terminal region of TEV) and CRY2PHR (cryptochrome 2 photolyase homology region)[20,21] (**Fig. 1a**).

TEV-C and TEV-N cannot bind each other in the absence of light (dark controls). In the presence of blue light, CRY2PHR and

[1]Max Planck Florida Institute for Neuroscience, Jupiter, Florida, USA. [2]Department of Anatomy, College of Medicine, Korea University, Seoul, Republic of Korea. [3]Department of Basic Neuroscience, University of Geneva, Geneva, Switzerland. [4]Service of Neurology, Geneva University Hospital, Geneva, Switzerland. [5]Max Planck Institute of Neurobiology, Martinsried, Germany. [6]Present address: University of Maryland School of Medicine, Baltimore, Maryland, USA. [7]These authors contributed equally to this work. Correspondence should be addressed to H.-B.K. (hyungbae.kwon@mpfi.org).

RECEIVED 27 JULY 2016; ACCEPTED 18 FEBRUARY 2017; PUBLISHED ONLINE 3 APRIL 2017; DOI:10.1038/NMETH.4234

CIBN interact, thereby causing TEV-C and TEV-N to interact, to regain protease function, and to cleave TEVseq. To avoid spontaneous TEVseq cleavage[23], we examined the crystal structure of the AsLOV2 protein, which shows that the Jα-helix is tightly associated with the Per-ARNT-Sim (PAS) core domain in the dark state but is released after blue-light illumination[24]. Thus, by replacing the C-terminal region of the Jα helix of AsLOV2 with TEVseq, we positioned TEVseq to prevent access by TEV protease in the dark state but to allow for complete access after blue-light illumination[22] (**Fig. 1a** and **Supplementary Fig. 1a**). To maximize the light inducibility of TEV protease from the dark state to the light state, we used a recently engineered AsLOV2, called improved light-inducible dimer (iLID)[22].

Using a secreted alkaline phosphatase (SEAP) assay, we tested several BLITz variants and found that BLITz-1 and BLITz-6 were the best light-induced constructs, each achieving over 20-fold-increased gene expression in response to blue-light illumination (**Supplementary Fig. 1**). Because the BLITz system relies on protein–protein interactions, fold changes varied depending on the ratio of individual modules (**Supplementary Fig. 2**). EGFP-reporter expression data corroborated the SEAP assay results (**Fig. 1b** and **Supplementary Figs. 3** and **4**), and we therefore selected BLITz-1 as our light-gating module.

Gene expression was also dependent on the duration of blue-light exposure. When a short light pulse (10 s on/50 s off) was repeated for 5 min, gene expression was significantly increased, and the fold change was dramatically increased with longer exposure times (**Fig. 1c**, one-way analysis of variance (ANOVA), $P = 0.064$ for TEVseq only; $P < 0.001$ for BLITz-1; $P < 0.001$ for BLITz-6; $P = 0.992$ for no tTA). Because the light cycle was 10 s on/50 s off per minute, only 50 s of total light exposure was sufficient to induce high gene expression, and 5 min of light stimulation induced changes in excess of 20 fold (**Fig. 1c**). Additionally, the light dependency conferred spatial resolution, thereby allowing us to limit EGFP expression to the cells exposed to blue light (**Fig. 1d**). Thus, we developed a light-inducible gene-coupled reporter system representing transitory protein interactions with a high SNR and precise spatiotemporal resolution.

Development of a light-inducible Tango platform

Unlike our BLITz system, the original Tango system lacks an external control switch[9], thereby resulting in cumulative activation of gene expression and therefore poor temporal resolution. We reengineered the original Tango system by combining it with the BLITz system, such that gene expression is initiated only when both ligand and light are present (**Fig. 2a**). In our *i*Tango system, ligand binding to receptors causes β-arrestin2-TEV-N recruitment but not TEVseq cleavage. Blue-light illumination then recruits CRY2-TEV-C to form a functional protease that cleaves TEVseq, thus leading to the release of the transcriptional activator and eventually to reporter-gene expression.

To verify that the *i*Tango system reliably detects neuromodulatory actions, we used the dopamine 2 receptor (D2R) transmembrane domain in the *i*Tango system. We expressed *i*Tango constructs in human embryonic kidney (HEK) 293T cells and introduced the D2R agonist quinpirole into the culture medium. In the dark control, there was no detectable spontaneous gene expression of the SEAP reporter, but after blue-light illumination, gene expression was dose dependent and was completely blocked by the D2R antagonist haloperidol (**Fig. 2b**). Notably, after transfection of a high titer of β-arrestin2-TEV-N plasmid, SNR robustly increased, thus suggesting that a reserve pool of β-arrestin2 protein in the cytosol is critical (**Supplementary Fig. 5**). An EGFP-reporter expression assay revealed the same quinpirole- and light-dependent pattern (**Fig. 2c**). These results indicated that gene expression was highly specific to D2R activation, and ligand-independent background signals were almost negligible, as expected from the two-step activation design. Thus, *i*Tango is a fast and reliable light-inducible technique, with a high SNR, that can be used to monitor neuromodulatory actions.

Optimization of *i*Tango for application to neurons

Next, we tested *i*Tango in neurons. To decrease the number of constructs, we generated a simplified version of *i*Tango called *i*Tango2, which lacks the CRY2PHR–CIBN light switch, thus allowing for efficient formation of the light- and ligand-induced protein complex (**Fig. 2d**). In *i*Tango2-transfected rat hippocampal culture neurons, background signals were nearly undetectable, whereas light and ligand inducibility were robust (**Fig. 2e** and **Supplementary Figs. 6** and **7**), with an SNR corresponding to an ~900% increase. (**Fig. 2f**). With the conventional Tango system, the same experiment yielded only a 50% increase in gene expression[25]. Thus, *i*Tango2 improved SNR ~20 fold over the classical Tango system in neurons.

We further tested spontaneous association of the split TEV system in the *i*Tango2 system. The original split TEV system is reportedly leaky[23,26]. Hence, restoration of TEV protease activity is partially independent of external signals such as pharmacological drugs or light. This leakiness may have originated from the intrinsic affinity of C- and N-terminal fragments or their tendency not to dissociate. This problem has been alleviated by use of a deletion mutant of TEV-C[26]. We used this truncated form of TEV-C in our *i*Tango system, but we further deleted its C terminus to minimize background levels. However, further deletion of three amino acids completely eliminated protease function, thus suggesting that the current truncated version of TEV-C is the smallest possible fragment that can lower the background level without causing a loss of intact protease activity (**Supplementary Fig. 8**).

To determine whether *i*Tango itself interferes with synaptic function, we transfected dopamine receptor 2 (DRD2)-*i*Tango2 constructs including β-arrestin2-TEV-C-P2A-TdTomato and TRE-EGFP reporter into mouse cortical pyramidal neurons in culture slices. Dendritic spines were counted from DRD2-*i*Tango2-transfected and neighboring nontransfected neurons to assess any changes in excitatory synaptic connectivity. The spine number was the same in the two populations, thus suggesting that the overall circuitry was not changed (**Supplementary Fig. 9**). We also measured α-amino-3-hydroxy-5-methyl-4-isoxazolepropionic acid (AMPAR)-mediated excitatory postsynaptic currents (AMPAR-EPSCs) evoked by two-photon uncaging at individual spines. The amplitude of AMPAR-EPSCs was normal in *i*Tango2-transfected neurons (**Supplementary Fig. 9**). Thus, the *i*Tango2 construct does not appear to cause major synapse or circuit dysfunctions.

Versatile application to other neuromodulators

Our modular design of the *i*Tango system allows for its use with other G-protein-coupled receptors and for creation of a library

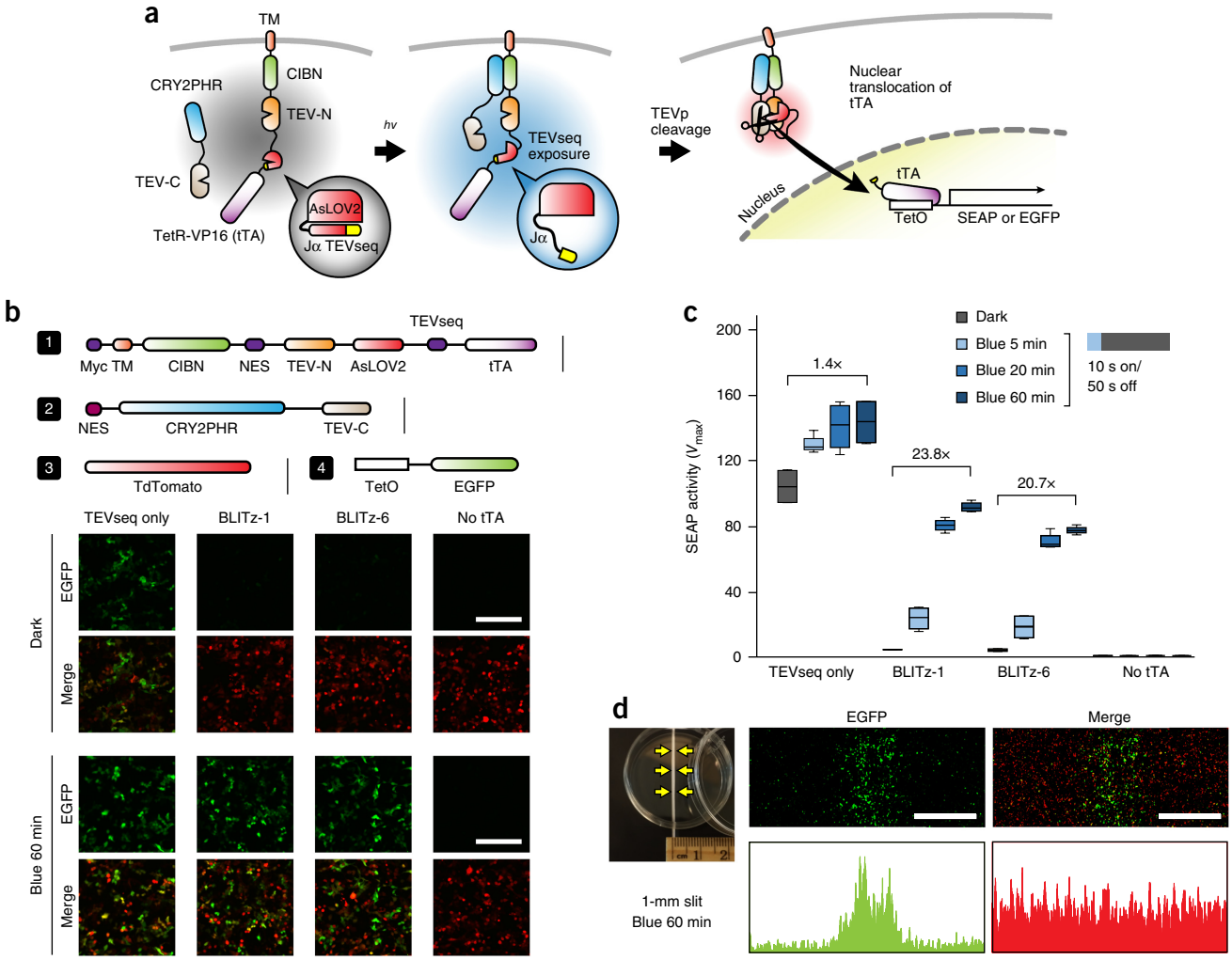

Figure 1 | Development of the BLITz system. (**a**) Schematic drawing of BLITz proteins and diagram of light-induced gene expression. TM, transmembrane domain; TetO, tetracycline operator. (**b**) Schematic of DNA plasmids transfected into cells (top). EGFP and TdTomato expression when different BLITz constructs were transfected (three independent transfections). NES, nuclear export signal. (**c**) Light-exposure-time-dependent gene expression fold changes. Data were averaged from six independent cultures. In the box plots, the upper whisker, middle, bottom, and lower whisker indicate the 10th, 25th, 50th, 75th, and 90th percentiles, respectively (one-way ANOVA, *post hoc* Games–Howell test). (**d**) Experimental setup using black masking tape (left). Representative images (of two total; middle, EGFP; right, merged image) of region-specific gene expression controlled by light. Scale bars, 200 µm (**b**) and 1 mm (**d**). DNA plasmids were transfected into HEK293T cells. Error bars, s.d.

of *i*Tango systems[12]. We constructed *i*Tango2 constructs fused to neuropeptide Y receptor type 1 (NPY1R), cannabinoid receptor type 1 (CB1R), and serotonin receptor 1A (5-HT_{1A}). Similarly to DRD2-*i*Tango2, NPY1R-*i*Tango2, CB1R-*i*Tango2, and 5-HT1A-*i*Tango2 showed light- and ligand-specific gene expression (**Fig. 2g–i** and **Supplementary Fig. 10**). Thus, *i*Tango2 is a versatile platform that allows for monitoring and manipulation of various neuromodulatory signaling events in the brain.

In vivo labeling of neuronal population sensitive to DA

To determine whether endogenous dopamine (DA) release is sufficient to trigger *i*Tango2-mediated gene expression *in vivo*, we injected AAV1-hSYN-DRD2-V2 tail-TEV-N-AsLOV2-tTA, AAV1-hSYN-β-arrestin2-TEV-C-P2A-TdTomato, and AAV1-hSYN-TRE-EGFP (short DRD2-*i*Tango2 viruses) bilaterally into the nucleus accumbens (NAc) and AAV-dFlox.hChR2(H134R)-mCherry into the right ventral tegmental area (VTA) in DAT-Cre mice (**Fig. 3a**). Under these conditions, coincident DRD2-*i*Tango2 activation and DA release were expected to occur only in the right hemisphere, but DRD2-*i*Tango2 in the left hemisphere was expected to remain a 'light only' control, because DA neuron projections are mostly unilateral[27]. As expected, blue-light illumination (10 s on/50 s off, 1 h) elicited robust EGFP expression exclusively in the right NAc (**Fig. 3b–d**). Minimal expression of EGFP in the left NAc confirmed that DRD2-*i*Tango2 constructs do not cause background signals without selective neuromodulator release (**Fig. 3c,d**). ChR2 expression in DA neurons was also confirmed in a posterior coronal section from the same mouse (**Fig. 3e**). These results indicated that DRD2-*i*Tango2 is sufficiently sensitive to detect endogenous phasic DA release *in vivo*. To determine the time course of induction and degradation of reporter-gene expression, we monitored EGFP expression after induction up to 10 d. The gene expression level peaked at 24–48 h and then slowly degraded over several days (**Supplementary Fig. 11**).

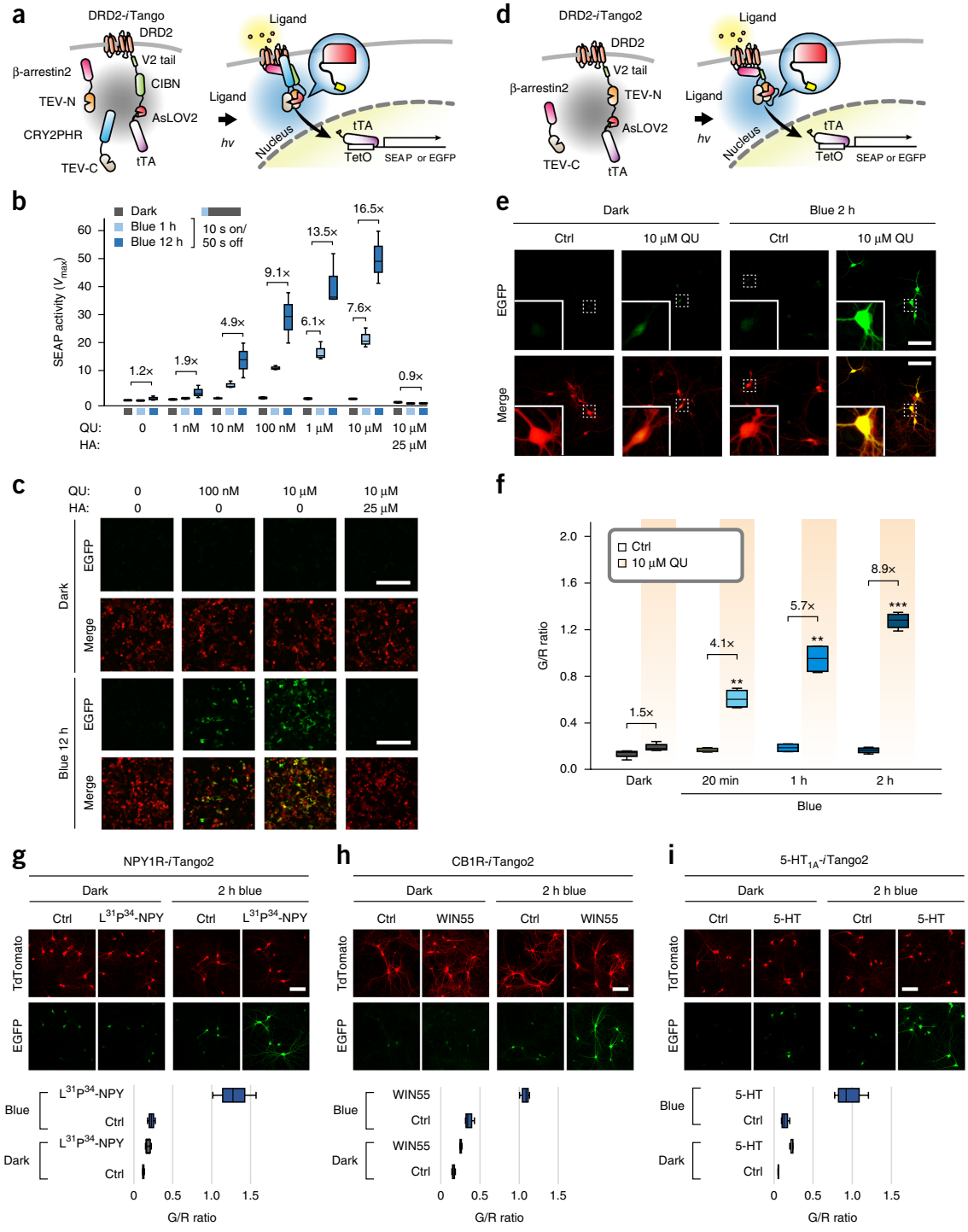

Figure 2 | Development of the *i*Tango platform. (**a**) Graphical illustration of the *i*Tango system. DRD2-V2 tail (C terminus of the V2 vasopressin receptor)-CIBN-AsLOV2-tTA functions as a main platform. (**b**) Gene expression levels, quantified by SEAP assays in HEK293T. The concentration of quinpirole (QU; ~1 nM–10 µM) and the period of blue light were varied (dark, blue 1 h, blue 12 h; three independent cultures). HA, haloperidol. (**c**) DRD2-*i*Tango system, monitored on the basis of EGFP expression. Scale bars, 200 µm. (**d**) Schematic design of the *i*Tango2 system. (**e**) Light- and ligand-dependent gene expression pattern tested in cultured rat hippocampal neurons. One representative neuron from each condition is magnified for clear visualization of expression. Scale bars, 100 µm. Ctrl, control. (**f**) Summary graph showing EGFP expression depending on the blue-light exposure time and DRD2 agonist quinpirole (10 µM). Gene expression was measured as the ratio of green to red fluorescence (G/R) intensities (one-way ANOVA, *post hoc* Games–Howell test, control versus 10 µM quinpirole; dark, 70 and 71 neurons; blue light 20 min, 69 and 66 neurons; blue light 1 h, 91 and 57 neurons; blue light 2 h, 65 and 79 neurons; four independent cultures). (**g**) NPY1R-sensitive *i*Tango2 tested in cultured hippocampal neurons. The selective NPY1R agonist [Leu31, Pro34]-neuropeptide Y (5 µg/ml) was added to cultured neurons in dark and light conditions. Representative images (of four total) of TdTomato (transfection marker) and EGFP expression (top). Summary graph of quantitative G/R ratio (bottom) (one-way ANOVA, *post hoc* Games–Howell test). (**h**) CB1R-*i*Tango2 test. Win55212-2 (10 µM) was used to activate. (**i**) 5-HT_{1A}-*i*Tango2 test. 50 µM of 5-HT was used to activate the 5-HT_{1A} receptor. Scale bar, 100 µm. $^{**}P < 0.01$; $^{***}P < 0.005$, respectively. Error bars, s.d.

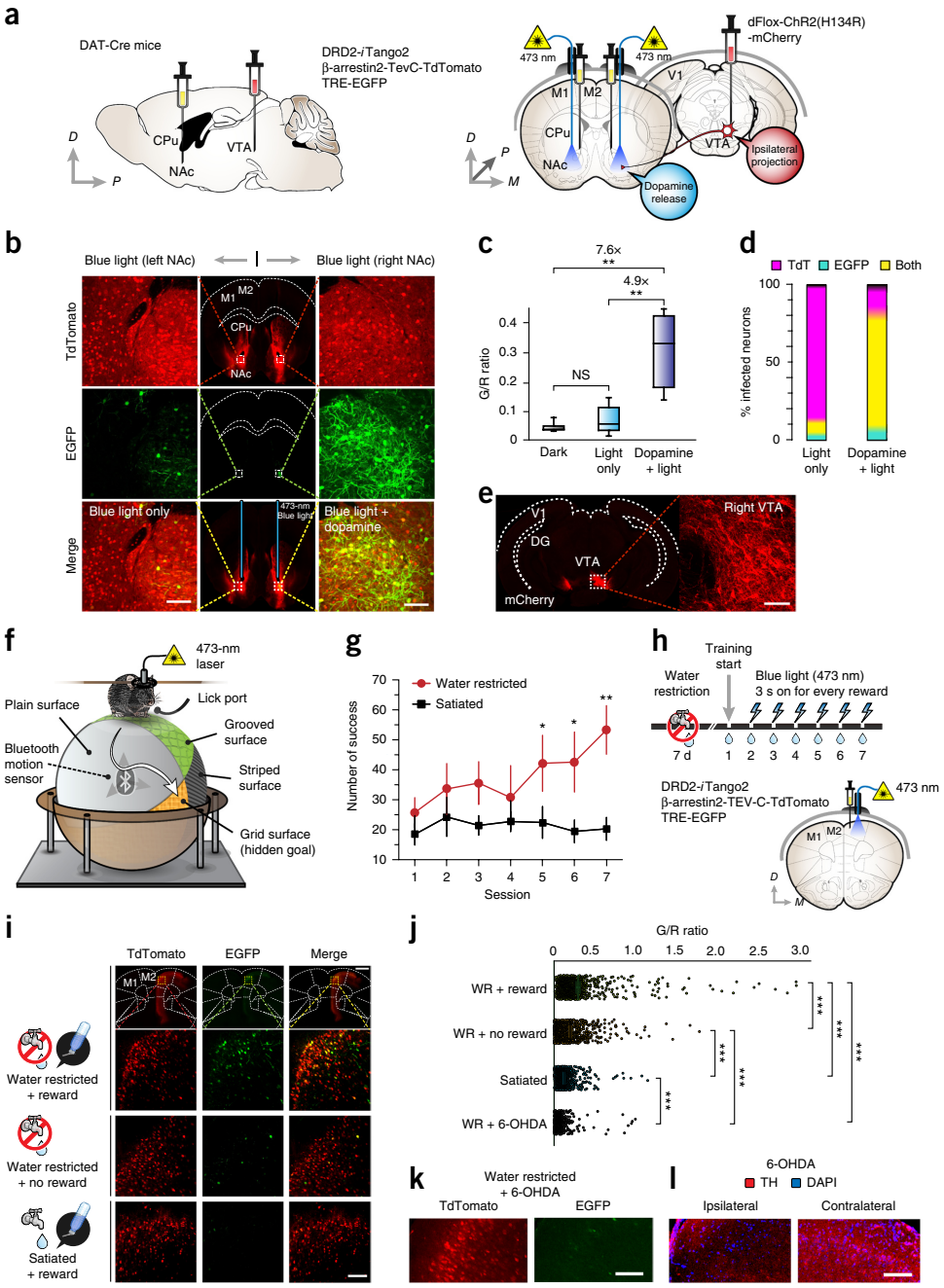

Figure 3 | *In vivo* labeling of the DA-sensitive neuronal population. (**a**) Schematic figure of viral injection. A mixture of DRD2-*i*Tango2 viruses including EGFP reporter were injected into left and right NAc areas in a DAT-Cre mouse. AAV-dFlox-ChR2(H134R)-mCherry was injected to the right side of the VTA area to selectively control DA release. Coronal-section view of viral injection and fiber-optic implantation. Both NAs were injected with *i*Tango2 viruses, and an optic fiber was implanted in both hemispheres. D, dorsal; P, posterial; M, medial. (**b**) Representative confocal images (of nine total) of DRD2-*i*Tango2 expression after exposure to blue light (10 s on/50 s off, 1 h). Red, green, and merged channel images are presented in the top, middle, and bottom rows, respectively. High-magnification images of the left and right NAc are presented for further clarification. (**c**) Summary graph of G/R ratio in the NAc (dark, 5 mice; light only, 6 mice; dopamine and light, 6 mice; *t* test, $^{**}P < 0.01$; NS, not significant). Boxes show the median, 25th and 75th percentiles, and whiskers show the 10th and 90th percentiles. (**d**) The percentage of red, green, and yellow positive neurons. Standard errors are indicated by gradient color at boundaries. (**e**) Coronal-section view of **b** from the same mouse. mCherry is expressed in DA-releasing neurons in the VTA region of DAT-Cre mice (left). High-magnification image of the VTA area (right). (**f**) Schematic drawing of the ball maze. Mouse movement was monitored by a Bluetooth motion sensor embedded in the center of the ball. (**g**) Graph showing the average numbers of water-reward successes. Animal training was performed for seven consecutive days (day 7; water restricted, 7 mice; satiated, 7 mice, Mann–Whitney *U* test, one sided, $P < 0.01$). (**h**) Timeline of the ball-maze experimental paradigm. (**i**) Representative TdTomato and EGFP signals from the M2 region after mice were subjected to the paradigm outlined in **h**. Yellow square boxes in the top images are magnified and presented in the bottom images. (**j**) Summary graph of G/R from individual neurons in water-restricted mice with and without rewards, satiated mice, and 6-OHDA-injected mice (water restricted with reward, 1,252 neurons, 7 mice; water restricted with no reward, 703 neurons, 7 mice; satiated, 892 neurons, 6 mice; water restricted with 6-OHDA, 452 neurons, 5 mice). (**k**) Representative M2-area images (of two total) from 6-OHDA-injected mice. 6-OHDA was administered when *i*Tango2 viruses were injected. (**l**) TH staining of the ipsilateral and contralateral side of M2 after 6-OHDA injection. Red signals indicate TH staining, and blue signals indicate DAPI nuclear staining. Scale bars are 100 μm in **b**, **e**, **i** (bottom), **k**, and **l**, and 1 mm in **i** (top). Error bars, s.e.m. $^{*}P < 0.05$; $^{***}P < 0.005$.

Visualization of a behaviorally relevant neuronal population with *i*Tango2

The feasibility of *i*Tango2 *in vivo* motivated us to test whether DRD2-*i*Tango2 could be used for identifying behaviorally relevant neuronal populations during specific animal behaviors. We first ensured that the target-gene expression was mediated by the concurrent presence of light and ligand. We illuminated rat hippocampal cultured neurons with blue light for 2 h and then applied quinpirole for 2 h. In this case, we did not detect a significant increase in double-positive (green and red) neurons (**Supplementary Fig. 12**; one-way ANOVA, $P > 0.05$). We next delivered light and reward concurrently or asynchronously in water-restricted mice with *i*Tango2 viruses injected in their NAc. In control mice, we delivered the light and ligand at a 90-s interval and repeated this cycle 20 times. Under this condition, we did not observe robust gene expression. In fact, the expression levels were significantly higher when light and reward were delivered coincidently (**Supplementary Fig. 12**, *t* test, two-tailed, $P < 0.05$ in comparison to asynchronous delivery; $P < 0.01$ in comparison to blue-light control; $P < 0.01$ in comparison to blue-light control). We also found that larger reward amounts caused higher levels of gene expression *in vivo* (**Supplementary Fig. 13**). Thus, our data verified that *i*Tango2-induced labeling requires the concurrent presence of light and ligand and is positively correlated with the amount of ligand *in vivo*.

To validate whether *i*Tango2 could be used to identify behaviorally relevant subsets of neurons, we trained mice in a simple ball maze. This setup was similar to the classical Morris water maze, but instead of visual cues, we added sensory cues on the surface of a Styrofoam ball, such that the mice would learn to associate one of the sensory cues with a reward. The ball was evenly divided into four sections, and the surface of each quadrant had one of four textures: plain, grooved, gridded, or striped (**Fig. 3f**). The reward spot was hidden at the center of the grid-surface section, so that whenever the mice reached the hidden spot, a water reward was provided, and the behavior was counted as a success. Water-restricted mice learned this task quickly over several days, as indicated by an increased number of successes per day (**Fig. 3g**). In contrast, the success rates did not increase when fully satiated mice were placed in the ball-maze setup (**Fig. 3g**). These results suggested that water-restricted mice were motivated to explore the ball and that the ball-maze task is a good method for assessing reward-based learning.

To identify the neuronal population activated by DA during this task, we injected DRD2-*i*Tango2 into the premotor cortex (M2) and shone blue light for 3 s whenever rewards were delivered (**Fig. 3h**). We conducted these experiments with water-restricted mice, satiated mice, and mice treated with 6-hydroxydopamine (6-OHDA), a neurotoxic compound that destroys dopaminergic projections. Two days after the last training session (day 7), we observed that the intensity of EGFP expression was significantly higher in water-restricted mice versus satiated mice or water-restricted mice with no reward (**Fig. 3i**,**j**, *t* test, $P < 0.001$). The group treated with 6-OHDA did not express EGFP, thus indicating that EGPF expression was induced by DA released at the time of reward delivery (**Fig. 3j**,**k**). The efficacy of 6-OHDA was also verified by staining with an antibody to tyrosine hydroxylase (TH) (**Fig. 3l**). Thus, the *i*Tango system enables the visualization of neuromodulation action with high spatiotemporal precision in awake behaving animals and can be used to identify DA-sensitive neuronal populations.

Labeling and manipulation of behaviorally relevant subpopulations of neurons in behaving animals

The *i*Tango system links gene expression to coincident stimulation by the presence of both a ligand and light, thereby enabling the manipulation of neuronal activity by optogenetic effectors. To determine whether *i*Tango could be used to establish causal effects of neuromodulators on neuronal circuits, we labeled two separate neuronal populations related to different behaviors. We injected DRD2-*i*Tango2 viruses and TRE-ChR2-EYFP into the central striatum and induced ChR2 expression in either locomotion- or reward-related neuronal populations that have recently been reported to be activated by DA[28] (**Fig. 4a**,**b**). We subjected mice to the ball-maze task as before and achieved selective ChR2 expression by illuminating the mice during either the locomotion phase or the reward phase (**Fig. 4b**,**c**). In a probe test, we then activated ChR2 via blue-light illumination in the neurons previously labeled with the *i*Tango system. In mice that had previously been subjected to illumination during the locomotion phase, ChR2 activation was sufficient to cause locomotion (**Fig. 4d**,**e**). When we labeled the reward-related neuronal population (reward-DA), the same blue light did not cause locomotion (**Fig. 4d**,**e**). Thus, *i*Tango2 is a useful tool to distinguish behaviorally relevant subpopulations of neurons in behaving animals and to test the sufficiency of eliciting behaviors.

Reversal of drug-induced locomotion sensitization with *i*Tango2

We also tested the *i*Tango2 system to influence circuits in a model of cocaine-induced locomotor sensitization. We used the D2-coupled DA-receptor sensing system to induce the expression of halorhodopsin (eNpHR), an amber-light-activated proton pump that inhibits cell firing (**Fig. 5a**). First, we confirmed that there was no expression of the AAV1-hSYN-Flox-β-arrestin2-TEV-C-P2A-TdTomato construct in Cre-negative cells, as indicated by an absence of signal in wild-type mice. We also confirmed that blue light was necessary to drive the expression of eNpHR-EYFP, because no EYFP signal was observed in the absence of blue light in all genotypes (**Fig. 5b**,**c**). Next, we took slices from the NAc of Cre-positive mice exposed to coincident blue light and cocaine, and used *ex vivo* slice electrophysiology to validate that 561-nm light inhibited firing of EYFP-positive cells (**Fig. 5d**). Finally, we performed a locomotor sensitization assay to demonstrate the functional relevance of this population of DA-sensitive NA neurons *in vivo*. After 3 d of habituation to the test apparatus, mice received an intraperitoneal (i.p.) injection of cocaine (20 mg/kg) paired with blue-light illumination, which induced a robust locomotor response (**Fig. 5e**,**f**). After 7 d of withdrawal, mice were returned to the test apparatus, and a challenge dose of cocaine was given. During this challenge, 561-nm light was applied for the duration of the behavioral measurement. Adaptations in D1-medium spiny neurons (MSNs) in the NAc have been implicated in the expression of locomotor sensitization to cocaine[29–32]. We selectively expressed the *i*Tango2 constructs in wild type, D1- or D2-Cre mice, to drive the expression of eNpHR in subpopulations that were responsive to cocaine-evoked DA release.

Optogenetic inhibition of the D1-MSN subpopulation during the cocaine challenge significantly suppressed the sensitized

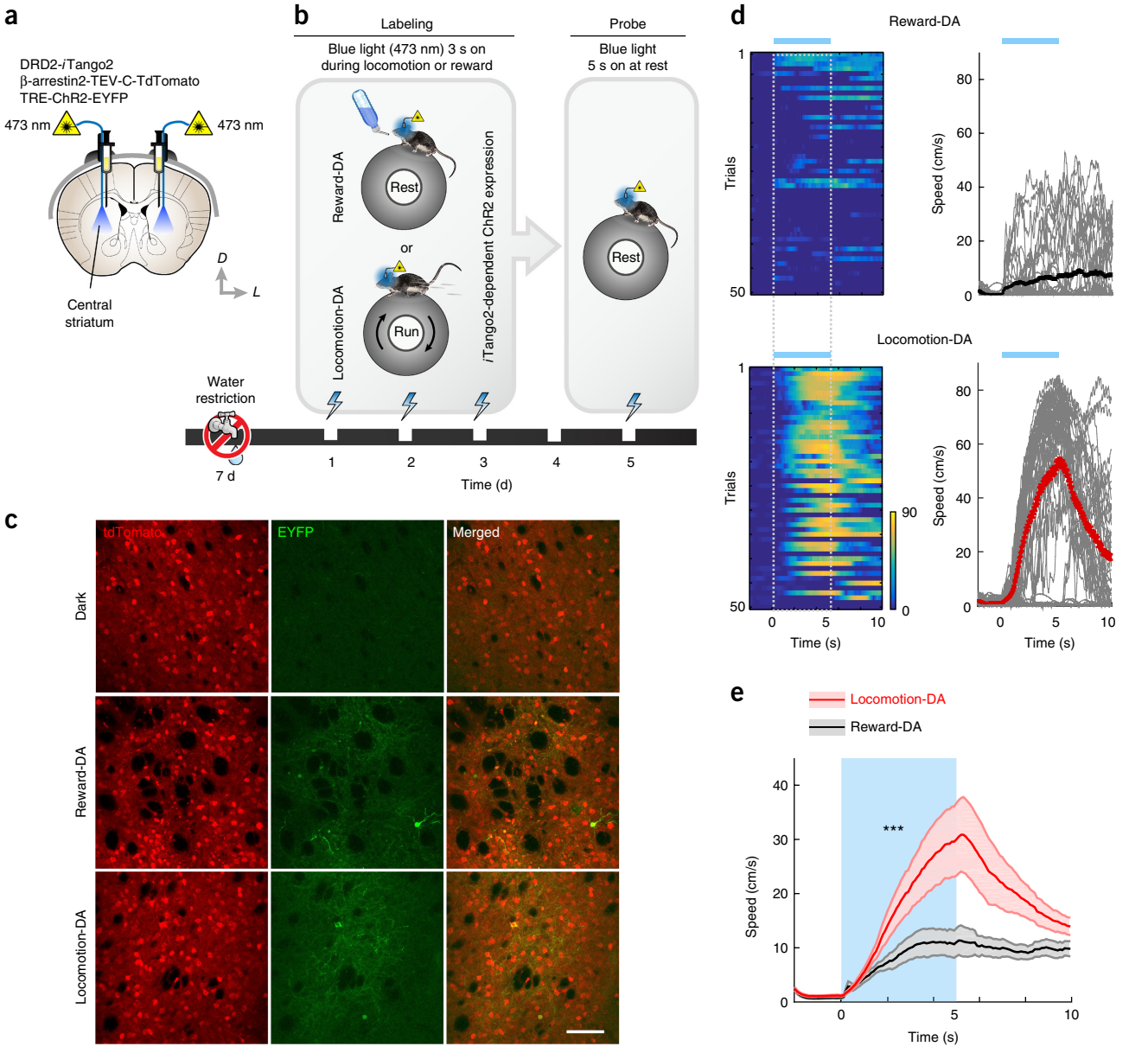

Figure 4 | *In vivo* manipulation of locomotion- and reward-related DA-sensitive neuronal populations in the central striatum. (**a**) Schematic of viral injection. (**b**) Graphical illustration of experiments. Blue light (473 nm) was delivered for 3 s when mice began locomotion (speed greater than 0.5 ms^{-1} for at least 2 s) or rest with a reward, for 50 trials per day over 3 d, to induce the expression of ChR2-EYFP reporter in locomotion- or reward-related DA-sensitive neuronal populations, respectively. Two days after induction, a probe test was conducted by delivering blue light when mice were at rest, to activate ChR2-expressing populations. (**c**) Coronal sections of the central striatum from mice not exposed to blue light (dark control, top), mice receiving blue light during rest with a reward (reward-DA, middle), and mice receiving blue light during locomotion (locomotion-DA, bottom). (**d**) Locomotion speed aligned on the basis of onset of laser stimulation (light blue) during a representative probe session from reward-DA (top) and locomotion-DA (bottom) groups. Each row represents a single trial from rest (left). Individual (thin gray line) and average (thick black and red) traces of locomotion speed over time are plotted (right). (**e**) Superimposed average speed of locomotion aligned to the onset of laser stimulation (light-blue box) from mice in the reward-DA and locomotion-DA groups (locomotion-DA, 6 mice; reward-DA, 6 mice; repeated-measures ANOVA, $F_{group \times time} = 5.58$, $^{***}P < 0.001$).

locomotor response to cocaine, whereas no effect was observed by manipulating DA-responsive D2-MSNs (**Fig. 5f**, two-way repeated-measures ANOVA, $P < 0.0001$ for Cre-negative, $P = 0.565$ for D1-Cre, $P = 0.006$ for D2-Cre). When cocaine administration occurred without light (dark control) or was asynchronized with light (light control), 561-nm light had no effect on locomotor sensitization (**Fig. 5g–j**). These results are consistent with the selective role of D1-MSNs in locomotor sensitization to cocaine and provide a proof of concept that the *i*Tango2 system can be used to manipulate and thus assess the behavioral relevance of a temporally and genetically identified population of neurons.

DISCUSSION

We developed a light-gated gene expression system named BLITz, a noninvasive and spatiotemporally precise gene expression system with low background signal. By implementing the BLITz system in the Tango system, we generated *i*Tango, a reporter for

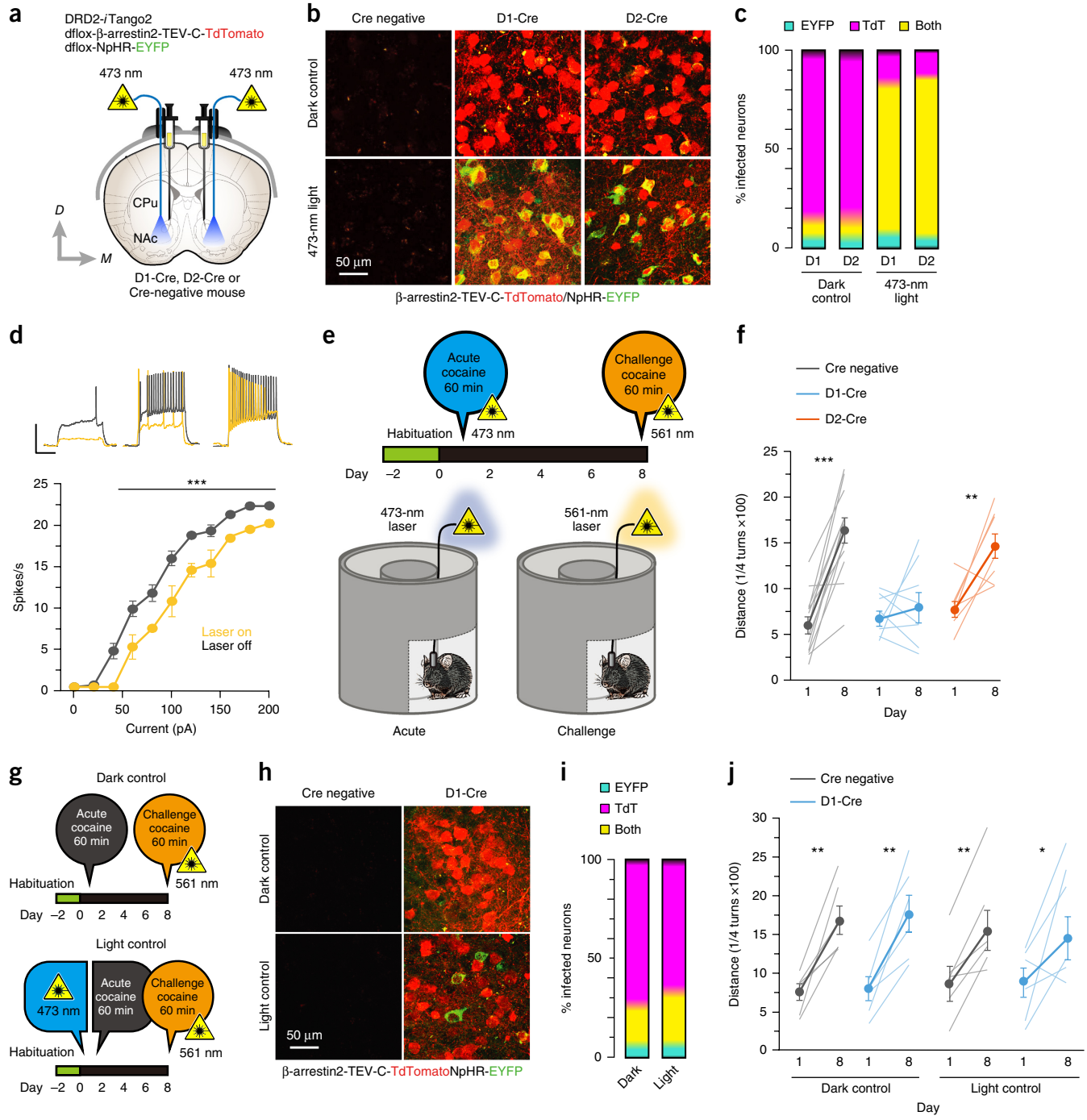

Figure 5 | *In vivo* manipulation of DA-sensitive neuronal populations in the NAc. (**a**) Schematic of viral injection. (**b**) Coronal sections of the NAc from Cre-negative (left), D1-Cre (middle), or D2-Cre (right) mice exposed to blue light (473 nm) for 60 min after a cocaine injection (bottom) or dark controls (top). (**c**) Quantification of infected neurons expressing EYFP or TdTomato alone, or coexpressing both fluorescent proteins (n = 6–8 mice per group in **b** and **f**). Standard errors are represented by gradient color at boundaries. (**d**) *Ex vivo* validation that amber light (561 nm) inhibits the spike activity of halorhodopsin-expressing MSNs (two-way repeated-measures ANOVA, $F_{current}$ = 1,325.42, P < 0.0001, F_{laser} = 90.73, P < 0.001, $F_{current \times laser}$ = 12.815, P = 0.03). (**e**) Schematic of experiment involving blue-light exposure with injection of cocaine (day 1) to induce the expression of halorhodopsin, which was subsequently activated with amber light during the cocaine challenge. (**f**) Locomotor activity of mice initially and after challenge with cocaine injection. Cre-negative mice showed robust sensitization to the challenge injection of cocaine (n = 13, P < 0.0001); this sensitized response was absent in D1-Cre mice (n = 8, P = 0.565), whereas D2-Cre mice (n = 8, P = 0.006) also showed robust sensitization ($F_{geneotype}$ = 39.86, P < 0.0001; $F_{geneotype \times time}$ = 7.96, P = 0.002). (**g**–**j**) Dark and light controls. (**g**) Schematic of experimental design. Dark controls received an injection of cocaine but were not exposed to light, whereas light controls were exposed for 60 min to blue light before the cocaine injection. (**h**) Coronal NAc sections from Cre-negative (left) and D1-Cre (right). Dark controls (top) or mice exposed to blue light for 60 min before cocaine injection (bottom). (**i**) Quantification of infected neurons expressing EYFP or TdTomato alone, or coexpressing both fluorescent proteins (n = 6 mice per group in **h** and **j**). Standard errors are represented by gradient color at boundaries. (**j**) Both dark controls (Cre negative, t_5 = 4.79, P = 0.005; D1-Cre, t_5 = 6.15, P = 0.002) and light controls (Cre negative, t_5 = 4.31, P = 0.008; D1-Cre, t_5 = 2.66, P = 0.045) exhibited a sensitized response to the second cocaine injection (n = 6 per group). *P < 0.05; **P < 0.01; ***P < 0.001.

ligand–receptor interactions. The improvement in spatiotemporal resolution and SNR over current methods allowed us to apply the *i*Tango technique to studies of the mammalian brain, in which subtle neuromodulatory signals were found to occur in a temporally precise manner. We showed that DRD2-*i*Tango2 can accurately identify neuronal populations sensitive to DA during reward-based learning. We used an *i*Tango system to express a proton pump that inhibits neuronal activity and showed that this construct inhibited cocaine-induced locomotor sensitization. *i*Tango2 may be useful in visualizing and manipulating the neuronal circuitry underlying drug-induced behaviors or other neuromodulation-related psychiatric diseases such as mood disorders or schizophrenia. In conclusion, *i*Tango2 is an optogenetic technique that links neuromodulatory actions to gene expression and substantially advances the ability to dissect the neural substrates of mammalian behavior.

METHODS

Methods, including statements of data availability and any associated accession codes and references, are available in the online version of the paper.

Note: Any Supplementary Information and Source Data files are available in the online version of the paper.

ACKNOWLEDGMENTS

We thank C. Tucker (University of Colorado) for CRY2 and CIBN constructs; B. Kuhlman (University of North Carolina, Chapel Hill) for the iLID construct; B. Roth (University of North Carolina, Chapel Hill) for NPY1R, CB1R, and 5-HT_{1A} constructs. K. Deisseroth (Stanford University) for the eNpHR-EYFP construct; R. Lefkowitz (Duke University) for the β-arrestin2 construct; S-Y. Choi (Chonnam National University) for the P2A vector; H. Zeng (Allen institute) for the TetO-EGFP construct; W. Weber (University of Freiburg) for the pSAM200 vector; and N. Gautam (Washington University in St. Louis) for the D2-YFP construct. We thank B. Lim (University of California, San Diego) for TRE-ChR2-EYFP viral production. We thank all members of the Kwon laboratory for critical discussion and support. This work was supported by funding from the Swiss National Science Foundation, the Academic Society of Geneva, the Private Foundation of the Geneva University Hospital, and a European Research Council Advanced Grant (MeSSI) (to C.L.); a Kil Chung Hee Fellowship (to D.L.); and the Max Planck Florida Institute for Neuroscience (to H.-B.K.).

AUTHOR CONTRIBUTIONS

D.L. and H.-B.K. conceived and initiated the project. D.L. designed and made DNA constructs. D.L. performed *in vitro* characterization and verification. D.L., K.J., and D.J.W. performed viral injection experiments in the NAc in DAT-Cre mice. M.C. and T.S. performed viral injection and cocaine-induced locomotion sensitization experiments. M.C. performed electrophysiology recording. K.J. performed behavioral training in the ball maze and the locomotion causality test. K.J. performed *in vivo* time-lapse analysis, differential reward-amount testing, time-offset experiments, and image analysis in the cortical M2 area. D.L., K.J., and D.J.W. performed viral injection and histological analysis. W.C.O. performed two-photon imaging and uncaging experiments combined with electrophysiology. N.L.M. provided assistance in DNA cloning. D.L., M.C., K.J., W.C.O., C.L., and H.-B.K. wrote the manuscript. All authors discussed and commented on the manuscript.

COMPETING FINANCIAL INTERESTS

The authors declare competing financial interests: details are available in the online version of the paper.

1. Barth, A.L. Visualizing circuits and systems using transgenic reporters of neural activity. *Curr. Opin. Neurobiol.* **17**, 567–571 (2007).
2. Chen, T.W. *et al.* Ultrasensitive fluorescent proteins for imaging neuronal activity. *Nature* **499**, 295–300 (2013).
3. Liu, X. *et al.* Optogenetic stimulation of a hippocampal engram activates fear memory recall. *Nature* **484**, 381–385 (2012).
4. Okuno, H. *et al.* Inverse synaptic tagging of inactive synapses via dynamic interaction of Arc/Arg3.1 with CaMKIIβ. *Cell* **149**, 886–898 (2012).
5. Anderson, D.J. & Adolphs, R. A framework for studying emotions across species. *Cell* **157**, 187–200 (2014).
6. Fu, Y. *et al.* A cortical circuit for gain control by behavioral state. *Cell* **156**, 1139–1152 (2014).
7. Posner, M.I. & Petersen, S.E. The attention system of the human brain. *Annu. Rev. Neurosci.* **13**, 25–42 (1990).
8. Barnea, G. *et al.* The genetic design of signaling cascades to record receptor activation. *Proc. Natl. Acad. Sci. USA* **105**, 64–69 (2008).
9. Inagaki, H.K. *et al.* Visualizing neuromodulation *in vivo*: TANGO-mapping of dopamine signaling reveals appetite control of sugar sensing. *Cell* **148**, 583–595 (2012).
10. Jagadish, S., Barnea, G., Clandinin, T.R. & Axel, R. Identifying functional connections of the inner photoreceptors in *Drosophila* using Tango-Trace. *Neuron* **83**, 630–644 (2014).
11. Kono, M. *et al.* Sphingosine-1-phosphate receptor 1 reporter mice reveal receptor activation sites *in vivo*. *J. Clin. Invest.* **124**, 2076–2086 (2014).
12. Kroeze, W.K. *et al.* PRESTO-Tango as an open-source resource for interrogation of the druggable human GPCRome. *Nat. Struct. Mol. Biol.* **22**, 362–369 (2015).
13. Eshel, N. *et al.* Arithmetic and local circuitry underlying dopamine prediction errors. *Nature* **525**, 243–246 (2015).
14. Herrero, J.L. *et al.* Acetylcholine contributes through muscarinic receptors to attentional modulation in V1. *Nature* **454**, 1110–1114 (2008).
15. Howe, M.W., Tierney, P.L., Sandberg, S.G., Phillips, P.E. & Graybiel, A.M. Prolonged dopamine signalling in striatum signals proximity and value of distant rewards. *Nature* **500**, 575–579 (2013).
16. Marlin, B.J., Mitre, M., D'amour, J.A., Chao, M.V. & Froemke, R.C. Oxytocin enables maternal behaviour by balancing cortical inhibition. *Nature* **520**, 499–504 (2015).
17. Tye, K.M. *et al.* Dopamine neurons modulate neural encoding and expression of depression-related behaviour. *Nature* **493**, 537–541 (2013).
18. Witten, I.B. *et al.* Cholinergic interneurons control local circuit activity and cocaine conditioning. *Science* **330**, 1677–1681 (2010).
19. Yagishita, S. *et al.* A critical time window for dopamine actions on the structural plasticity of dendritic spines. *Science* **345**, 1616–1620 (2014).
20. Kennedy, M.J. *et al.* Rapid blue-light-mediated induction of protein interactions in living cells. *Nat. Methods* **7**, 973–975 (2010).
21. Wehr, M.C. *et al.* Monitoring regulated protein-protein interactions using split TEV. *Nat. Methods* **3**, 985–993 (2006).
22. Guntas, G. *et al.* Engineering an improved light-induced dimer (iLID) for controlling the localization and activity of signaling proteins. *Proc. Natl. Acad. Sci. USA* **112**, 112–117 (2015).
23. Williams, D.J., Puhl, H.L., III & Ikeda, S.R. Rapid modification of proteins using a rapamycin-inducible tobacco etch virus protease system. *PLoS One* **4**, e7474 (2009).
24. Harper, S.M., Neil, L.C. & Gardner, K.H. Structural basis of a phototropin light switch. *Science* **301**, 1541–1544 (2003).
25. Djannatian, M.S., Galinski, S., Fischer, T.M. & Rossner, M.J. Studying G protein-coupled receptor activation using split-tobacco etch virus assays. *Anal. Biochem.* **412**, 141–152 (2011).
26. Gray, D.C., Mahrus, S. & Wells, J.A. Activation of specific apoptotic caspases with an engineered small-molecule-activated protease. *Cell* **142**, 637–646 (2010).
27. Oades, R.D. & Halliday, G.M. Ventral tegmental (A10) system: neurobiology. 1. Anatomy and connectivity. *Brain Res.* **434**, 117–165 (1987).
28. Howe, M.W. & Dombeck, D.A. Rapid signalling in distinct dopaminergic axons during locomotion and reward. *Nature* **535**, 505–510 (2016).
29. Creed, M., Pascoli, V.J. & Lüscher, C. Addiction therapy: refining deep brain stimulation to emulate optogenetic treatment of synaptic pathology. *Science* **347**, 659–664 (2015).
30. Lobo, M.K. & Nestler, E.J. The striatal balancing act in drug addiction: distinct roles of direct and indirect pathway medium spiny neurons. *Front. Neuroanat.* **5**, 41 (2011).
31. Pascoli, V., Turiault, M. & Lüscher, C. Reversal of cocaine-evoked synaptic potentiation resets drug-induced adaptive behaviour. *Nature* **481**, 71–75 (2011).
32. Robinson, T.E. & Berridge, K.C. Addiction. *Annu. Rev. Psychol.* **54**, 25–53 (2003).

ONLINE METHODS

Design and construction of plasmid vectors. Construction sequences are fully described in **Supplementary Data**. A schematic illustration of each construct is provided in **Supplementary Figure 14**. To generate CMV::TM-CIBN-NES-TEV-N-BLITz-1-tTA, we amplified CIBN, AsLOV2, and tTA sequences from pCIBN (ΔNLS)-pmGFP (gift from C. Tucker, Addgene 26867), pLL7.0: Venus-ILID-CAAX (gift from B. Kuhlman, Addgene 60411), and pSAM200 (gift from W. Weber), respectively. Amplified PCR products were digested by a suitable combination of restriction enzymes, and each PCR product was cloned into a synthesized TEV-N backbone. CMV::NES-CRY2PHR-TEV-C was generated by ligating synthesized TEV-C backbone and amplified CRY2PHR from Pcry2PHR-mCherryN1 (gift from C. Tucker, Addgene 26866). CMV::HA-DRD2-V2 tail-CIBN-BLITz-1-tTA was produced by a series of ligations of V2 tail, AsLOV2-tTA, and DRD2. The sequence encoding the HA signal and V2-tail backbone originated from PRESTO-Tango sequences, except for modification of several restriction-enzyme sites[12]. DRD2 was amplified from pcDNA3.1-D2-YFP (gift from N. Gautam) with BamHI and EcoRI sites. We produced CMV::β-arrestin2-TEV-N-P2A-TdTomato with a simple subcloning method. β-arrestin2 sequence was amplified from β-arrestin GFP WT (gift from R. Lefkowitz, Addgene 35411). For the generation of reporter AAV vector, pTRE-FLEX-EGFP-WPRE-bGHpA (gift from H. Zeng, Addgene 65449) was used as a backbone vector. The floxed-eNpHR-EYFP sequence was acquired from pAAV-double floxed-eNpHR-EYFP-WPRE-pA (gift from K. Deisseroth, Addgene 20949). ChR2(H134R) sequence was cloned from pAAV-EF1a-double floxed-hChR2(H134R)-mCherry-WPRE-HGHpA (gift from K. Deisseroth, Addgene 20297). All cloning enzymes and reagents were purchased from New England BioLabs. All plasmid vectors generated in this study were reconfirmed by DNA sequencing (Eurofin Genomics).

Site-directed mutagenesis for BLITz constructs. To generate BLITz variants, we inserted or deleted small nucleotides from the original AsLOV2 sequence through site-directed mutagenesis. Whole amplification of the vector was performed with KOD polymerase (71086-3, EMD Millipore), which allows for high-speed, accurate PCR amplification. To remove parental templates, we used DpnI (R0176, New England BioLabs) restriction enzyme at 37 °C for 1 h. This mixture was directly added to competent cells (*E. coli* DH5α strain, Zymo Research). Primers used for mutagenesis are described in **Supplementary Data**.

HEK293T cell culture and DNA transfections. HEK293T cells were purchased from the American Type Culture Collection (ATCC) and were tested for mycoplasma contamination. HEK293T cells were grown in high-glucose Dulbecco's Modified Eagle's Medium (DMEM) (Gibco) containing 10% FBS (10438-018, Gibco) and 1% penicillin–streptomycin (Invitrogen). HEK293T cells were chosen because they can be readily transfected and result in reliable quantitative assays. In addition, HEK cells do not express neuronal ion channels or receptors and consequently provide a suitable environment to detect changes mediated by exogenously transfected constructs. Cells were incubated at 37 °C and 10% CO_2 conditions. For the experiments, all dishes and coverslips were precoated with 1 mg/ml poly-D-lysine hydrobromide (P0899, Sigma-Aldrich) solution for 2 h. After being treated with 0.25% trypsin (25200, Gibco) for 2 min, detached cells were collected, and the total cell numbers were counted. Dissociated cells were plated with 2×10^5 cells per 12-mm coverslip. 24 h later, DNA plasmid vectors were transfected with a Calcium Phosphate Transfection Kit (Clontech). The mixture of DNA solution was slowly added into 2× HEPES-buffered saline. After a 1-h incubation, precipitated solutions were added into the wells.

Preparation of dissociated hippocampal culture and DNA transfections. Primary hippocampal neuron culture was performed as previously described[33]. Briefly, CD IGS rat hippocampus (embryonic day 18) (Charles River, strain code 001) was rapidly dissected and digested with 0.25% trypsin-EDTA (Invitrogen) for 10 m at 37 °C. After trypsin-EDTA was removed, the trypsinized cells were carefully triturated with a 1,000-μL pipette tip ten times. Dissociated cells were counted, and 10^5 cells were plated onto 12-mm PDL-coated coverslips. The plating medium consisted of neurobasal medium (Invitrogen) and the following reagents; 1% (vol/vol) FBS, 1% (vol/vol) Glutamax supplement (Gibco), 2% (vol/vol) B27 supplement (Gibco), and 1% (vol/vol) penicillin–streptomycin. Primary hippocampal neuron cultures were grown at 37 °C and 10% CO_2 conditions. Every 4 d, one-third of the media volume was replaced with fresh maintenance medium lacking FBS. DNA was transfected with the neuronal calcium phosphate transfection method, as previously described[34]. Three days later (DIV 10), cells were illuminated with a short period of blue light for 2 h (5 s on/55 s off), and quinpirole and/or haloperidol was added into the medium when necessary. After a 2-h incubation, the medium was replaced with fresh medium. Neurons were fixed at DIV 12 for imaging acquisition.

Blue-light illumination for neuron culture. Blue-light illumination was performed with a 465-nm-wavelength blue LED array (LED Wholesalers) that was controlled by a high-accuracy digital electronic timer (model 451, GraLab). The LED array was installed inside a 37 °C, 10% CO_2 incubator. One transparent blank plate with a 2-cm height was inserted between the LED source and the sample to inhibit potential undesirable heating caused by direct contact with the LED. In our experimental setup, the power of blue light at the specimen was 1.7 mW, as measured with a power meter (PM100D, ThorLabs). For the dark condition, all light was blocked by wrapping of culture plates in aluminum foil, and experimental procedures were carried out under dim red light.

Two-color flow cytometry analysis of HEK293T. HEK293T cells were harvested with 0.25% trypsin-EDTA. After centrifugation, cells were washed and resuspended in FACS buffer (PBS with 2% FBS). We analyzed dissociated cells (10,000 cells per sample) on a FACSCanto II instrument (BD Biosciences). Dead cells and debris were excluded from the analysis population with forward- and side-scatter parameters. For the detection of EGFP and TdTomato, we used a 488-nm argon laser and 530/30-nm and 585/42-nm band-pass filters, respectively. To avoid spillover between EGFP and TdTomato, we adjusted the acquisition parameters through a compensation process, by using three transfection controls (EGFP only, TdTomato only, and no transfection).

doi:10.1038/nmeth.4234

All FACS data were acquired and processed with FACSDiva software (version 6.1.3).

SEAP chemiluminescence assay. For the quantification of gene expression, we used secreted embryonic alkaline phosphatase (SEAP) chemiluminescent assays. All reagents for the SEAP assays were purchased from InvivoGen. Forty-microliter samples were collected from the medium in each well and transferred into 96-well plates. Samples were preheated in a 60 °C incubator for 10 min to inhibit the activity of endogenous alkaline phosphatase. All mixtures were added into a single master tube containing SEAP substrates and L-homoarginine. Mixed solutions were carefully added into each sample in 96-well plates, to avoid bubbles. The chemiluminescence of each sample was measured with a microplate reader (SpectraMax Plus 384, Molecular Devices) at 37 °C and 405 nm. Assays were performed every 30 s for 2 h. All data acquisition and V_{max} calculations were performed with SoftMax Pro 5.4.1 (Molecular Devices).

Preparation and transfection of cortical organotypic slice cultures. Organotypic slice cultures from the mouse somatosensory cortex were prepared from P3–P4 C57BL/6 mice[35] in accordance with the Institutional Animal Care and Use committee of the Max Planck Florida Institute for Neuroscience and the National Institutes of Health guidelines and were transfected through biolistic gene transfer (180 psi) 6 or 7 d before imaging[36]. Five micrograms of DRD2-*i*Tango2, 10 μg of β-arrestin2-TEV-C, and 5 μg of TRE-EGFP were coated onto 6–7 mg of gold particles.

Two-photon imaging and glutamate uncaging on organotypic slice cultures. Imaging and uncaging were performed at 13 or 14 d *in vitro* (DIV) on transfected or nontransfected layer-2/3 pyramidal neurons within 40 μm of the slice surface at room temperature in recirculating artificial cerebrospinal fluid (ACSF; 127 mM NaCl, 25 mM $NaHCO_3$, 1.25 mM NaH_2PO_4, 2.5 mM KCl, and 25 mM d-glucose, aerated with 95%O_2/5%CO_2) with 2 mM $CaCl_2$, 1 mM $MgCl_2$, 2.5 mM MNI-glutamate, and 0.001 mM TTX. For each neuron, image stacks (512 × 512 pixels; 0.048 μm/pixel) with 1-μm *z* steps were collected from one segment of secondary or tertiary apical dendrites with a two-photon microscope (Prairie Technologies) with a pulsed Ti::sapphire laser (Mai Tai, Spectra Physics) tuned to 930 nm (2–2.5 mW at the sample). To record uncaging-evoked excitatory postsynaptic currents (uEPSCs), layer-2/3 neurons were patched in whole-cell voltage-clamp configuration (MultiClamp 700B amplifier (Molecular Devices), V_{hold} = −65 mV, electrode resistance 5–8 MΩ) with a cesium-based internal solution (135 mM Cs-methanesulfonate, 10 mM HEPES, 10 mM Na_2 phosphocreatine, 4 mM $MgCl_2$, 4 mM Na_2-ATP, 0.4 mM Na-GTP, 3 mM Na l-ascorbate, and 0.2 mM Alexa 488; ~300 mOsm, pH ~7.25) in ACSF. uEPSC amplitudes from individual spines were quantified as the average (8–10 test pulses of 1-ms duration at 0.1 Hz) from a 2-ms window centered on the maximum current amplitude after uncaging pulse delivery. Laser pulses were delivered by parking the beam at a point ~0.5 μm from the center of the spine head (720 nm; 16–18 mW at the sample).

Quantification of densities and fluorescence intensities of dendritic spines. All distinct protrusions emanating from the dendritic shaft, regardless of shape, were counted and measured in images from the green (Alexa 448) channel with ImageJ (NIH). The estimated spine volume was measured from background-subtracted green-fluorescence intensities by using the integrated pixel intensity of a boxed region of interest (ROI) surrounding the spine head, as previously described[37].

Cell preparation and acquisition of images. Cells were fixed with prewarmed 4% paraformaldehyde (Santa Cruz Biotechnology) for 10–15 min. Fixed cells were rinsed with PBS three times. Coverslips were mounted with mounting solution (Electron Microscopy Science). Imaging was performed with an upright confocal laser-scanning microscope (LSM780, Zeiss) with a 20×/0.8 M27 objective lens.

Animals. C57BL6J mice (males and females 3–6 weeks old, Jackson Laboratory) were used. For selective manipulation of DA neuron activity, DAT-IRES-Cre (DAT-Cre) heterozygous mice (3–6 weeks old, Jackson Laboratory stock 006660) were used. The genotypes of DAT-Cre mice were confirmed by PCR-based genotyping (common primer, 5′-TGG CTG TTG GTG TAA AGT GG-3′; wild-type reverse primer, 5′-GGA CAG GGA CAT GGT TGA CT-3′; mutant reverse primer, 5′-CCA AAA GAC GGC AAT ATG GT-3′; mutant band size, 152 bp; wild-type band size, 264 bp). For locomotor sensitization experiments, D1-Cre (Tg(Drd1-cre)EY262Gsat/Mmucd) and D2-Cre (Tg(Drd2-cre)ER44Gsat/Mmucd) heterozygous mice (6–10 weeks of age) were used[38]. We did not use a method of randomization for selecting animals. Animals were allocated into experimental groups in a non-blinded manner. All experimental procedures and protocols were approved by the Max Planck Florida Institute for Neuroscience Institutional Animal Care and Use Committee and complied with the National Institutes of Health guidelines and the University of Geneva guidelines for animal care. No statistical method was used to predetermine sample size.

Adenoassociated viral constructs. All *i*Tango AAV constructs were cloned in the laboratory, and viruses were produced at ViGene Bioscience. The viral titers of constructs were: AAV1-hSYN-DRD2-*i*Tango2, 1.37×10^{14} GC/mL; AAV1-hSYN-β-arrestin2-TEV-C-P2A-TdTomato, 2.57×10^{14} GC/mL; AAV1-hSYN-Flox-β-arrestin2-TEV-C-P2A-TdTomato, 2.44×10^{14} GC/mL; AAV1-TRE-EGFP, 2.30×10^{14} GC/mL; and AAV1-TRE-Flox-eNpHR-EYFP, 1.65×10^{14} GC/mL. Flox-ChR2-mCherry was purchased from the Penn vector core. AAV-TRE-ChR2-EYFP was produced by B. Lim's laboratory (University of California, San Diego).

Animal surgery and stereotactic viral injection. AAV viral solutions were injected into mouse brains in a stereotactic setup (Kopf instruments). Before craniotomy, mice were fully anesthetized with a cocktail of ketamine (80 mg/kg) and xylazine (12.5 mg/kg) (Sigma-Aldrich) via i.p. injection. The hair of each mouse was cleanly removed with hair-remover lotion (Nair, Church & Dwight), and petrolatum ointment (Puralube Vet Ophthalmic Ointment) was administered to both eyes to relieve dry eyes. Next, mice were fixed to a stereotactic device by using both an ear bar and a nose clamp, and the surgical region was scrubbed with 10% betadine solution (Purdue Product LP). During

surgery, the mouse body temperature was maintained at a constant 37 °C with a homeothermic blanket with a flexible probe (Harvard Apparatus). After the level of anesthesia was checked, the head skin and periosteum were carefully removed with sharp surgical scissors and a scalpel under aseptic surgical conditions. The imaginary line between the bregma and lambda was adjusted to maintain horizontality. To make a small burr hole (~0.5-mm diameter) in the mouse skull for viral injection, we used a handheld drill (Fordom Electric Co.) under a surgical microscope. Premixed viral solution (AAV1-hSYN-DRD2-*i*Tango2, AAV1-hSYN-β-arrestin2-TEV-C-P2A-TdTomato, and AAV1-TRE-EGFP in a 2:2:1 ratio, injection volume, 700 nl) and dFlox-ChR2-mCherry viral solution (Penn Vector Core; injection volume, 500 nl) were injected via a pulled glass micropipette connected to a syringe pump device (World Precision Instruments). The injection flow rate was controlled within the range of ~100–200 nl/min. For microinjection, glass micropipettes (tip size 10–20μm diameter, Braubrand) were fabricated with a micropipette puller (P-1000, Sutter Instruments), and the tip of each micropipette was beveled with a micropipette grinder (EG-400, Narishige). We determined injection coordinates on the basis of a preliminary injection trial with fast green dye and the Mouse Brain Atlas (http://mouse.brain-map.org/static/atlas/). The following coordinates were used. Nucleus accumbens. AP, +1.4 mm; ML, ±1.5 mm from the bregma; DV, −4.0 mm from the brain surface. M2 area, AP, +1.75 mm; ML, +0.3 mm from the bregma; DV, −0.25 mm from the brain surface. VTA, AP, −3.25 mm; ML, +0.5 mm from the bregma; DV, −4.0 mm from the brain surface. After injection, the micropipette was held in place for 3 min to prevent backflow of viral solutions. For ball-maze training, custom-made headplates were attached to the exposed skull with dental adhesive.

Fabrication and implantation of optic fiber. An optic fiber (low OH, 200-μm core, 0.37 NA; BFL37-2000, Thorlabs) was cut with a diamond knife and inserted into a 1.25-mm-diameter ceramic ferrule (CFLC230-10, Thorlabs) with a 230-μm bore. The optic fiber was adhered to the ferrule with epoxy (Gorilla Glue Company). Both ends of the optic fiber were finely ground with polishing sandpaper and a grinding puck (Thorlabs). After viral injection, the optic fiber was implanted perpendicularly into the targeted brain region under the guidance of stereotactic device and a cannula holder (XCL, Thorlabs). To secure the implanted optic fiber, dental cement (C&B-Metabond, Parkell) was applied to the skull surface. After complete solidification of the dental cement, the cannula holder was removed from the implanted optic fiber. Finally, analgesic (buprenorphine, 0.05 mg kg^{-1} body weight) was injected subcutaneously to relieve postsurgical pain, and mice were returned to their home cages for recovery.

Mouse training in a ball maze. Mice were allowed to recover from viral injection and optic-fiber-implantation surgery for ~18–25 d before being trained to perform a tactile-based spatial navigation task on a custom-made spherical-floating-ball maze. Mice in the water-restricted group were limited to 1 ml water per day for 7 d before the start of training. Mice in the satiated group were given *ad libitum* access to water and were additionally given 2 ml of 10% sucrose solution 30 min before each training session. The floating-ball maze was made of an air-supported 8-inch-diameter spherical Styrofoam ball, each quadrant of which featured a plain, grooved, stripped, or grid texture. A simple auditory tone (8 kHz for 2 s) was delivered at the beginning and end of training. During navigation, movement of the mice was monitored with a CMOS camera (Thorlabs), and ball movement was continuously monitored with a Bluetooth motion sensor (LPMS-B, LP Research) placed at the center of the ball and was recorded in MATLAB (Mathworks). Mice were trained to find an unmarked goal location (surface area of 30° solid angle) that triggered delivery of a reward of 10% sucrose solution (~10 μl). The reward was delivered via a lick port positioned directly in front of the mouse's mouth, and delivery timing was controlled with a solenoid valve (NResearch). Brief air puffs (60 psi, 200 ms) were directed at the hind limbs after 30 s of inactivity to encourage continuous exploration of the ball maze. To prevent excessive access to the goal, a refractory period was assigned to the lick port, such that revisits to the goal location within 3 s of a reward did not trigger another reward. Labeling of the stable reward-related neuronal population was accomplished by the delivery of blue light (473 nm; ~10–30 mW) through the optic fiber for 3 s after each reward from training session 2. The behavioral setup was controlled with a custom-written code in MATLAB (Mathworks). Daily training sessions lasted 800 s for 7 d.

Blue-light delivery *in vivo*. Mice were allowed to recover from viral injection and optic-fiber-implantation surgery for ~18–25 d before undergoing optogenetic manipulation. Blue light generated by a 473-nm laser (MBL-FN-473, Changchun New Industries Optoelectronic Technology) at ~10–30 mW power was delivered to the animals for 10 s on/50 s off (**Fig. 3a–d**) or 30 s on/30 s off (**Fig. 5**) for 1 h through an optic fiber (200-μm core, 0.37 NA, Thorlabs); the timing of light delivery was controlled by a custom code written in MATLAB (Mathworks).

Labeling of the reward- or locomotion-sensitive neuronal population. *i*Tango2 viruses with ChR2-EYFP reporter were injected bilaterally into the central striatum (AP, +1.1 mm; ML, ±1.5 mm from the bregma; DV, −2.5 mm from the brain surface). Mice were allowed to recover from viral injection and optic-fiber-implantation surgery for ~18–25 d before being trained to perform a behavioral task on an air-supported spherical treadmill. Mice were limited to 1 ml water per day for 7 d before training and were pseudorandomly assigned into two experimental groups. Animals in group 1 received a reward of 10% sucrose solution (~10 μl) when they rested (no speed greater than 0.05 ms^{-1} for at least 2 s). Labeling of the neuronal subpopulation sensitive to dopamine during the reward was accomplished by the delivery of blue light (473 nm; ~10–30 mW) through the optic fiber for 3 s in synchrony with each reward. For animals in group 2, labeling of the neuronal subpopulation sensitive to dopamine during locomotion was accomplished by the delivery of blue light (473 nm; ~10–30 mW) through the optic fiber for 3 s during locomotion (speed greater than 0.5 ms^{-1} for at least 2 s). Each light delivery was considered to be a trial. The minimum time interval between trials was 30 s. The animals were monitored with a CMOS camera (Thorlabs), and locomotion was continuously recorded in MATLAB (Mathworks) with a Bluetooth motion sensor (LPMS-B, LP Research) placed at the center of the ball. The behavioral setup was controlled with a custom-written code in MATLAB (Mathworks). Training comprised 50 trials per day for 3 d. At 2 d

doi:10.1038/nmeth.4234

after the end of training, a probe test was conducted by delivery of blue light (473 nm, 10 mW, 5 s) to the mice when they rested. The probe test consisted of 50 trials.

Locomotor sensitization experiments. The sensitization apparatus consisted of two concentric tubes of 30- and 10-cm diameters forming a circular corridor. The position of the mouse was tracked from below by using AnyMaze software. Mice were allowed to recover from viral injection (AAV1-hSYN-DRD2-*i*Tango2, AAV1-hSYN-Flox-β-arrestin2-TEV-C-P2A-TdTomato, and AAV1-TRE-Flox-eNpHR-EYFP in a premixed 2:2:1 ratio) and optic-fiber-implantation surgery for ~18–25 d before being habituated to the sensitization apparatus. For 3 d of habituation, mice received an injection of saline and were placed in the apparatus for 60 min. On day 1 of cocaine exposure, mice were allowed to acclimate to the apparatus for 20 min before receiving a 20 mg/kg i.p. injection of cocaine, and locomotor activity was tracked for the following 60 min. During the 60 min after cocaine administration, mice received blue-light stimulation (473 nm, 30 s on/30 s off) through a bilateral optic-fiber cannula implanted over the NAc. After 7 d of withdrawal, mice received a challenge dose of cocaine in an identical procedure, except that orange light (561 nm) was administered to activate halorhodopsin.

***Ex vivo* electrophysiology.** Coronal brain slices (210 µm) were prepared in cooled artificial cerebrospinal fluid containing 119 mM NaCl, 2.5 mM KCl, 1.3 mM $MgCl_2$, 2.5 mM $CaCl_2$, 1.0 mM Na_2HPO_4, 26.2 mM $NaHCO_3$, and 11 mM glucose, bubbled with 95% O_2 and 5% CO_2. Slices were kept at 30–34 °C in a recording chamber superfused with 2.5 ml/min artificial cerebrospinal fluid. Visual whole-cell recording techniques were used to measure the holding and synaptic responses of eNpHR-EYFP positive neurons in the NAc. The internal solution contained 130 mM CsCl, 4 mM NaCl, 5 mM creatine phosphate, 2 mM $MgCl_2$, 2 mM Na_2-ATP, 0.6 mM Na_3-GTP, 1.1 mM EGTA, and 5 mM HEPES. In current clamp configuration, 1-s current steps were injected in increments of 20 pA from 0 pA to 200 pA, and the numbers of spikes were quantified in the presence and absence of 561 nm wavelength light.

Slice preparation. Animals were deeply anesthetized with a mixture of ketamine and xylazine and then perfused transcardially, first with PBS, pH 7.4, then with 4% paraformaldehyde (PFA) dissolved in PBS. The brains were removed and postfixed in 4% PFA overnight at 4 °C. The brains were embedded in 10% melted gelatin solution for 50 min at 50 °C, and then the gelatin solution was refreshed, and the embedded brains were incubated in 4 °C for ~30 min to allow for gel solidification. Then the gel was trimmed into a small cube around the brain, and the cube was placed in 4% PFA overnight. The gelatin-embedded brains were coronally sectioned (100 µm thick) with a vibratome (Leica Biosystems). Cells were analyzed with a confocal microscope (Zeiss LSM880).

Immunohistochemistry. Mice were deeply anesthetized with a mixture of ketamine and xylazine and then perfused transcardially, first with PBS, pH 7.4, then with 4% PFA dissolved in PBS. The brains were removed and postfixed in 4% PFA overnight at 4 °C and then cryoprotected in 30% sucrose in PBS at 4 °C for 2–3 d. The brains were coronally sectioned (40 µm thick) with a vibratome (Leica Biosystems). Tyrosine hydroxylase (TH) staining was accomplished as follows: 40-µm-thick slices were rinsed three times in PBS, pH 7.4; slices were blocked in 10% normal goat serum for 1 h; incubated with rabbit polyclonal anti-TH primary antibody (1:700 in PBS; Sigma, cat. no. T8700) for 24 h at 4 °C; rinsed in PBS three times; incubated in Cy3-conjugated goat anti-rabbit IgG (1:100 in PBS, Jackson ImmunoResearch Laboratories, cat. no. 111-165-003) for 2 h at room temperature on a rotary shaker; rinsed in PBS three times and mounted with DAPI Fluoromout-G (Southern BioTech). Antibody validation is available on the manufacturers' websites. TH-positive fibers in the cortex were imaged with a confocal microscope (Zeiss LSM880).

Pharmacology. Quinpirole, haloperidol, [Leu31,Pro34]-neuropeptide Y, Win55212-2, and 5-HT were purchased from Tocris Bioscience. All drug stock solutions were prepared at 1,000× concentrations or greater. Cocaine hydrochloride was obtained from the University of Geneva pharmacy and diluted to a concentration of 2 mg/ml in 0.9% saline.

Statistics. The statistical significance of cell culture data was calculated with one-way ANOVA with *post hoc* Games–Howell test in SPSS 12.0 (IBM) software. Comparison of G/R in *in vivo* experiments and behavioral changes during the ball-maze test was performed with nonparametric Mann–Whitney (one-sided) tests. Single, double, and triple asterisks indicate $P < 0.05$, $P < 0.01$, and $P < 0.005$, respectively. Electrophysiological validation of halorhodopsin data was analyzed with repeated-measures ANOVA with laser on or off as the between-subject variable and the current step as the within-subject variable. Locomotor sensitization data were analyzed with a repeated-measures ANOVA with genotype as the between-subject factor and time point as the within-subject factor, and were subsequently analyzed with paired *t* tests.

Data availability. The data supporting the findings of this study are available from the corresponding author upon reasonable request. Source data for **Figures 1–4** are available online. Key plasmids and their sequences are available from Addgene (no. 74021).

33. Lee, D. *et al.* Inositol 1,4,5-trisphosphate 3-kinase A is a novel microtubule-associated protein: PKA-dependent phosphoregulation of microtubule binding affinity. *J. Biol. Chem.* **287**, 15981–15995 (2012).
34. Jiang, M. & Chen, G. High Ca^{2+}-phosphate transfection efficiency in low-density neuronal cultures. *Nat. Protoc.* **1**, 695–700 (2006).
35. Stoppini, L., Buchs, P.A. & Muller, D. A simple method for organotypic cultures of nervous tissue. *J. Neurosci. Methods* **37**, 173–182 (1991).
36. Woods, G. & Zito, K. Preparation of gene gun bullets and biolistic transfection of neurons in slice culture. *J. Vis. Exp.* (12), 675 (2008).
37. Oh, W.C., Hill, T.C. & Zito, K. Synapse-specific and size-dependent mechanisms of spine structural plasticity accompanying synaptic weakening. *Proc. Natl. Acad. Sci. USA* **110**, E305–E312 (2013).
38. Gerfen, C.R., Paletzki, R. & Heintz, N. GENSAT BAC cre-recombinase driver lines to study the functional organization of cerebral cortical and basal ganglia circuits. *Neuron* **80**, 1368–1383 (2013).